CLM-R 232

CLM-R 232

UKAEA

Report

PREDICTED BEHAVIOUR OF THE PUMPED LIMITER OF INTOR

M. F. A. HARRISON
E. S. HOTSTON

CULHAM LABORATORY
Abingdon Oxfordshire

1982

C/18 Available from H. M. Stationery Office £2.00

CLM-R232

PREDICTED BEHAVIOUR OF THE PUMPED LIMITER OF INTOR

M F A Harrison and E S Hotston

Culham Laboratory, Abingdon, Oxon OX14 3DB, UK
(Euratom/UKAEA Fusion Association)

September 1982

Abstract

Modelling of the pumped limiter envisaged for INTOR Phase IIA predicts that an effective exhaust of helium can be attained with a pumping speed of about 100 $m^3 s^{-1}$ provided that the power flow to the under-surfaces of a tungsten limiter plate is not less than about 6 MW. This requirement is likely to be compatible with a tip loading of 1 MW m^{-2}. Plasma characteristics below the limiter plate are sensitive to the exhaust speed of the vacuum system and it is advantageous to maintain a relatively low pumping speed.

Assessment of the performance of tungsten and beryllium limiter plates shows that the sputter rate of tungsten is low (typically < 1 cm/year) and that self-sputtering is not likely to be a problem even if the charged particle input power is as high as 40 MW. Sputter erosion of the beryllium plate is large ($\approx$ 20 cm/year) and the helium exhaust pumping requirements for beryllium are about twice as demanding as those for tungsten. In neither case is there evidence of significant atomic radiation cooling by impurity ions which recycle in the immediate vicinity of the plate.

Consideration of the scrape-off plasma provides evidence that localised recycling of DT ions in the immediate vicinity of the limiter is a significant transport mechanism when the scrape-off plasma density is $\gtrsim 10^{19}$ m^{-3}. The charged particle power flow necessary to maintain this recycling is at least 4 MW and, since energy is carried to the sheath predominantly by electron conduction along the magnetic field, there is a substantial temperature gradient between the sheath regions at the limiter plate and the bulk of the scrape-off plasma. The temperature at the separatrix distant from the plate may therefore be in excess of 50 eV.

September 1982

ISBN 0 85311 117 0

1. Introduction

The objective of this paper is to predict the performance of the pumped-limiter configuration envisaged for INTOR Phase IIA[1] using models for plasma transport parallel to the magnetic field in the scrape-off region. Modelling techniques for plasma and gas transport are based upon those developed for the single-null divertor[2,3] but the method of their application has been altered to allow for the limiter geometry and also to take account of the sensitivity of limiter performance to radial variation of the plasma parameters within the scrape-off region. There are at present considerable uncertainties regarding both the radial characteristics of the scrape-off plasma and the dimensions and precise location of the limiter plate; therefore the physical behaviour of the system has been assessed over a relatively wide range of operating conditions in the general regime of a medium density scrape-off, eg, $n \sim 5 \times 10^{19}\ m^{-3}$ at the separatrix.

Radial transport codes (see for example Ref.4) predict that a stable radiative plasma edge will form inboard of the separatrix in cases where the limiter surface is composed of iron or tungsten. The power carried by charged particles through the scrape-off plasma to the limiter is then low (eg, $\sim$ 10 MW) and some preliminary assessments of pumped-limiter performance[5,6] have been obtained. However, if the limiter is constructed from low atomic number material such as beryllium, then radiative power losses are small and about 80 MW flows to the limiter in INTOR. Thus a further objective of the present work is to contrast the impurity release and gas exhaust properties of beryllium and tungsten pumped-limiters.

2. Modelling of the Pumped Limiter

2.1 Topology of the plasma transport region

The pumped limiter configuration envisaged during Phase IIA of the INTOR workshop consists of a toroidally symmetric plate located at the bottom of the torus; the concept is illustrated here in Fig.1. Plasma drifts to the upper and lower surfaces of the plate but, because of the mushroom shape of the limiter cross section, neutral particles formed by ion impact upon the upper surface tend to move preferentially towards the separatrix*. They contribute to recycling of

*The term separatrix is used here to describe the surface of closed magnetic field that grazes the innermost portion of the limiter surface.

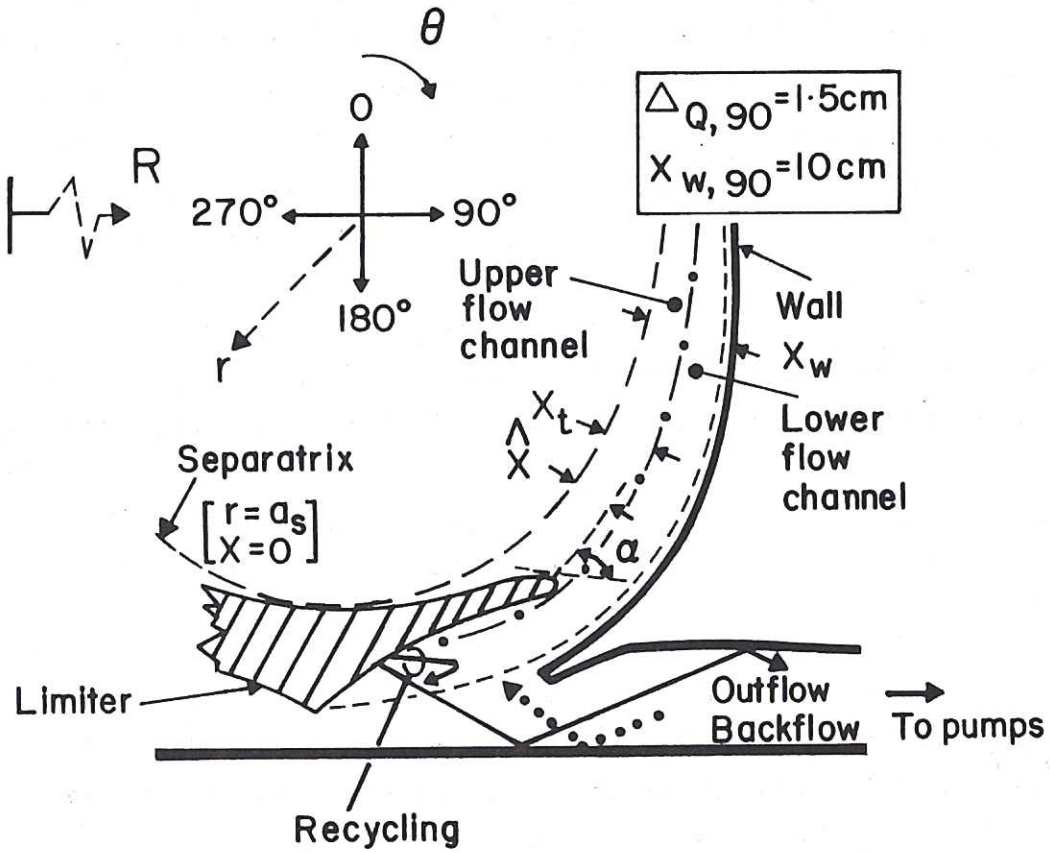

Fig.1 Concepts adopted in modelling the pumped limiter as viewed in the poloidal plane. The poloidal magnetic field configuration is taken from Ref.7 and only the outer portion of the limiter plate is shown.
For present purposes it is assumed that the total area of the upper surface is about $40\,m^2$ and this surface is shaped so as to provide an approximately uniform power loading. The peak power loading close to the tip is $\approx 1\,MW\,m^{-2}$. Other parameters are discussed in the text.

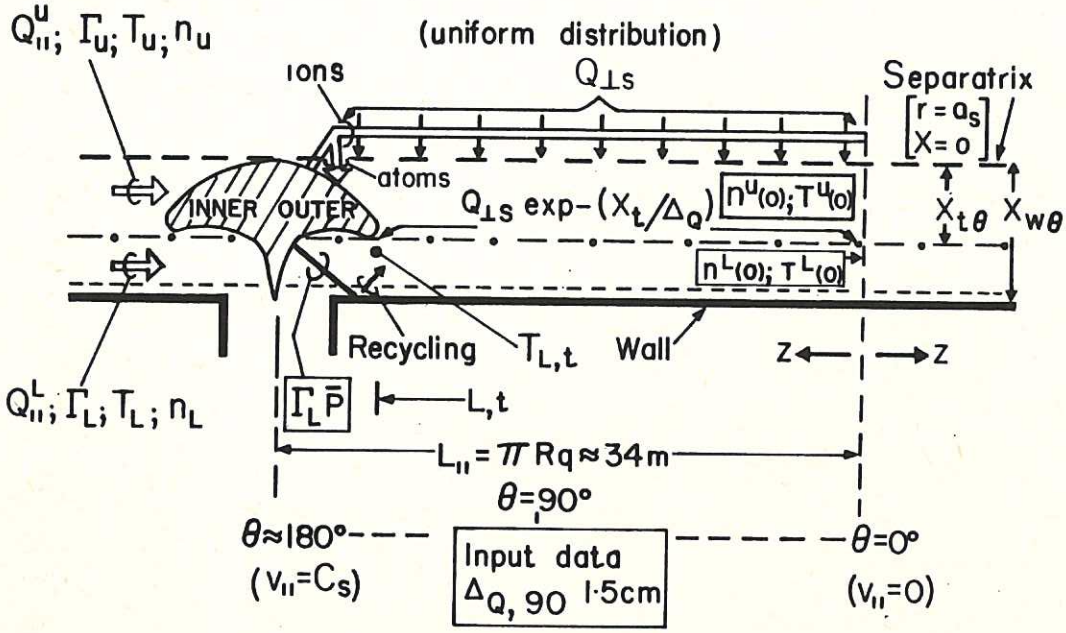

Fig.2 Concepts adopted for modelling plasma and gas transport within the scrape-off region and close to the limiter surface. The illustration represents a linear projection of the transport channels and boundary surfaces in the direction parallel to the magnetic field. The limiter is toroidally symmetric but to aid presentation it is here illustrated by its cross section which has been oriented normal to the field. The radial flow of energy $Q_{\perp}$ is balanced by a parallel flow $Q_{\parallel}$ in the scrape-off plasma, the flow rate of charged particles is Γ and the plasma drift length is $L_{\parallel}$. The configuration is symmetric about z = 0 (i.e. the total transport is $2Q_{\parallel}$, 2Γ, etc.) and the terms "inner" and "outer" are used to distinguish the major radii of the limiter surfaces. Conditions at the limiter surface are identified by the sub or superscript U or L depending upon whether they relate to the upper or lower surface and the corresponding parameters at z = 0 are identified by (0).
Other parameters are either illustrated in Fig.1 or discussed in the text.

particles and energy across the separatrix but they have little effect upon the exhaust of gas by the pumps. By contrast, neutral particles released from the lower surface move preferentially towards the torus wall and the pump ducts and so these are the predominant source of neutral exhaust gas. Modelling procedures previously used to study the divertor are based upon one-dimensional flow of plasma parallel to the direction z of the magnetic field in the scrape-off region. In the case of the limiter, it is necessary to consider two flow channels; one which feeds the upper surface of the plate and the second which feeds the lower surface. This concept is illustrated in Fig.2.

Plasma transport within the scrape-off region is modelled using a circular geometry equivalent to the INTOR configuration. It is postulated that transport occurs along channels in which the effective drift length of the plasma, $L_{||}$, is equal to half of the length of the magnetic flux tubes that link the "inner" and "outer" faces of the limiter*, ie,

$$L_{||} \approx \pi R_o q(r) \qquad (1)$$

where R_o is the major radius of the plasma axis and q(r) is the "equivalent circular" safety factor at minor radius r.

Radial transport across the magnetic field feeds energy into the scrape-off plasma and the amount transported by charged particles, $Q_{\perp}(r)$; is assumed, (a) to be uniformly distributed along the drift length $L_{||}$ of the channel and (b) to flow equally towards the inner and outer faces of the limiter. The power flow from the plasma to the scrape-off region is thus $2Q_{\perp s}$ where the subscript s refers to the separatrix at $r = a_s$.

2.2 Radial transport of plasma particle energy

The present 1-D fluid model of plasma transport parallel to the magnetic field in the scrape-off region does not permit a self-consistent estimation of the radial profile of plasma transport associated with charged particles. As a consequence, an exponential profile based

*Inner and outer in respect to the toroidal plane, ie, inner lies at the smaller major radius.

upon the recommendations in Ref.1 is used, namely,

$$Q_{\perp}(X) = Q_{\perp s} \exp - \frac{X}{\Delta_Q} \qquad (2)$$

where X is the radial distance outboard of the separatrix and Δ_Q is a radial scale length for energy transport. Further, the model does not allow for power losses due to atomic radiation and charge exchange inboard of the separatrix or during the drift time of the plasma that crosses the separatrix and moves towards the limiter plate. Approximate allowance for these losses can be made by suitable adjustment of the charged particle input power $Q_{\perp s}$ and so limiter performance is assessed for a range of input powers. The likely operational regime can therefore be identified by cross reference to the input powers derived from radial modelling of the plasma (see, for example, Ref.4).

The model implies that the radial decrement in $Q_{\perp s}$ is exactly balanced by flow of energy along the field towards the limiter so that the power, $Q_{||}(X)$, transported towards the limiter by plasma lying between $r = a_s$ and $r = (a_s + X)$ is given by

$$Q_{||}(X) = Q_{\perp s} \int_0^X \exp - \frac{X}{\Delta_Q} dX \ . \qquad (3)$$

The average power loading of the surface is thus given by

$$\Psi_Q(X_\theta) \approx \sin \alpha \frac{Q_{\perp s}}{2\pi R_\theta \Delta_{Q\theta}} \exp - \frac{X_\theta}{\Delta_{Q\theta}} \qquad (4)$$

where α is the angle at which the limiter surface is inclined to the intersecting magnetic surface (see Fig.1). The dependence of X_θ, R_θ and $\Delta_{Q\theta}$ upon poloidal angle θ is introduced to account for the localised effects of non-circular geometry of both the limiter and the plasma.

Engineering requirements[1] impose limits upon the acceptable peak power loading, $\hat{\Psi}_Q$, which should not exceed about 1 MW m^{-2} in the region close to the tip. Thus it is necessary to displace the tip outboard of the separatrix in the manner illustrated in Fig.1 where the displacement $\hat{X}$ corresponds to the allowed peak power load. The shape of the limiter tip and the thickness of the plate are not yet specified and so in the present paper it is assumed that the radius of curvature of the tip is negligible compared to Δ_Q so that $\hat{X} \approx X_t$ where X_t is the

displacement of both the tip and the lower surface of the plate. The power transported by charged particles towards the upper surface can thus be expressed as

$$Q_{||}^{U} = Q_{\perp s} \int_{o}^{X_{t,\theta}} \exp - \frac{X_\theta}{\Delta_{Q,\theta}} \, dX \tag{5}$$

whereas that transported towards the lower surface is given by

$$Q_{||}^{L} = Q_{\perp s} \int_{X_{t,\theta}}^{X_{w,\theta}} \exp - \frac{X_\theta}{\Delta_{Q,\theta}} \, dX. \tag{6}$$

Here $X_{w,\theta}$ is the local spacing between the separatrix and torus wall.

2.3 Atomic loss processes close to the limiter plate

Although the distant effects of atomic processes are not assessed directly the model does account for local effects of atomic and surface interactions on both the upper and lower surfaces of the plate. Treatment of energetic atoms, radiation and self-sputtering are described in Refs.2 and 3. It is assumed when determining atomic losses that a negligibly small number of sputtered impurities escape from the locality of the limiter; this condition also applies to DT that recycles to the lower surface of the plate but not so for DT which recycles at the upper surface. These aspects are discussed in Section 2.5.

2.4 Transport parallel to the magnetic field

Modelling of plasma transport for conditions of collisional flow parallel to the magnetic field within the scrape-off region and also for convective flow through the plasma sheath at the limiter surface is described in Refs.2 and 3. Transport in the scrape-off region is assessed by using an equivalent circular geometry so that the effective area of the flow channels in the direction normal to z can be expressed as

$$[A_{||}]_Q \approx \frac{2\pi a_s \Delta_s}{q_s} \approx 0.145 \text{ m}^2. \tag{7}$$

Here $q_s = 2.1$ is the safety factor at the circular separatrix of INTOR and $\Delta_s \approx 2\Delta_{Q,90}$ where $\Delta_{Q,90} = 1.5$ cm is taken from the specification[(1)] for the mid-outer toroidal plane, ie, at $\theta = 90^o$ where $q_{90} \approx 1$.

To model the flow it is also necessary to specify either the density n(o) or the temperature T(o) in the upstream region of the scrape-off plasma (ie, at the position z = 0 in the channels shown in Fig.2) Finite thermal conductivity parallel to the magnetic field implies that T(o) is rather insensitive to $Q_{||}$ and so the scrape-off density n(o) is the more significant parameter. Thus, $n^U(o)$ and $n^L(o)$ are chosen as prescribed input parameters for modelling flow in the channels that feed the upper and lower surfaces of the limiter. In the present model the flow channels are treated independently in the sense that no account is made for the interchange of plasma particles between them and the input energies are apportioned according to eqs.(5) and (6).

2.5 Gas transport

At the limiter surface, the limiter plate acts as a material barrier for particle exchange. Neutral particles produced by plasma impact upon the upper surface are either ionised locally within the flow channel and recycled as ions to the surface or else they escape across the separatrix surface. The escaping particles eventually return to the scrape-off region either as daughter atoms of charge exchange collisions or else as outward diffusing plasma ions. The returning ions are assumed to be uniformly distributed over the surface of the separatrix whereas the daughter atoms are assumed to be localised to the upper surface of the plate.

Neutral particles released from the lower surface move preferentially towards the torus wall and pumping ducts. The gas exhaust properties are treated in the same manner as for the divertor[3] on the assumption that the limiter will be mounted upon a pumping cassette of comparable geometry. In steady state, the release rate of neutral particles at the lower surface of the limiter equals the flow rate Γ_L of plasma ions to this surface and the rate of exhaust of neutral gas of atomic species J from the lower surface of the limiter can therefore be expressed as

$$\Gamma^{(o)}_{J(pump)} = 2\left[\frac{\Gamma_L \overline{P} F}{(1 - (1 - F)R)}\right]_J \qquad (8)$$

where the factor 2 is based upon the assumption that the inner and outer faces of the limiter contribute equally to gas exhaust. Here $\overline{P}_J$ is the probability that neutral particles can escape from the lower plasma channel and F_J is the efficiency with which the flow of directly escaping neutrals $[\Gamma_L\overline{P}]_J$ (see Fig.2) is exhausted from the outlet of the

vacuum pumps. Thus F_J is governed by the total speed S_J of the pumps and also by the gas transport properties of the ducts. R is a reflection coefficient that allows for the recycling of neutral particles between the plasma channel and the local surfaces of the torus wall and pumping ducts.

The power input to the lower drift channel $Q_{||}^{L}$ is relatively small due to the constraints imposed by the restriction on power loading at the limiter tip. The temperature T_L of the plasma at the sheath edge of the lower surface (ie, at $z = L_{||}$) may therefore be so low that the mean free paths of atomic processes under the limiter become comparable to the radial extent of the plasma channel (ie, $\approx \Delta_{Q,\theta}$) and also to the scale length for the temperature gradient in the z direction (ie, $[dT/dz]_L$). Consequently, R and the radiation and charge exchange power losses are determined at an average plasma temperature, $\overline{T}_L$, given by

$$\overline{T}_L = \frac{\int_o^{(z = L_t)} T(z)dz}{\int_o^{(z = L_t)} dz} \approx \frac{7}{9} T_{L,t} + \frac{2}{9} T_L \qquad (9)$$

where $T_{L,t}$ is the temperature of the plasma channel of length $z = L_t$ where it passes below the tip of the limiter (see Fig.2). Application of eq.(9) shows that backflowing neutral particles are likely to be ionised in the region below the limiter plate.

3. General Behaviour of the Pumped Limiter

3.1 Upper surface

A limiter and divertor differ substantially in the sense that the impurity source arising from plasma bombardment of the limiter plate or divertor target is, in the case of the limiter, not separated from the separatrix surface. Consequently the limiter is likely to act as a more prolific source of impurity ions that may radiate inboard of the separatrix and thereby reduce the power transported by charged particles to the scrape-off plasma. Nevertheless, within the context of charged particle transport, the characteristics in the sheath and flow channel to the upper surface of the limiter will differ but slightly from those predicted for a divertor subjected to the same input power. An indication of the behaviour of the divertor for input powers ranging from 20 to 100 MW can be found

in Refs.2 and 3. The principal difference predicted by the present model is that the plasma temperature, T_U, at the sheath edge tends to be higher than that for comparable conditions within the divertor. This is predominantly a consequence of the relatively small effective area $[A_{||}]_Q$ of flow to the limiter plate. (The flow area in the divertor is enhanced by inward diffusion across the magnetic field within the divertor chamber, see Refs.2 and 3.)

3.2 Lower surface

Conditions at the sheath and in the flow channel are appreciably different from those at the upper surface. The input power $Q_{||}^L$ is always low because of the engineering constraints imposed upon the peak power loading at the tip, namely,

$$Q_{||}^L \approx 2\pi R_\theta \Delta_{Q,\theta} \hat{\Psi}_Q, \tag{10}$$

which for INTOR yields $Q_{||}^L \not> 3$ MW for $\hat{\Psi}_Q = 1$ MW/m^2. In these conditions, the plasma temperature T_L at the sheath edge may be sufficiently low to change the balance between energy lost by convective transport through the sheath to the limiter plate and that needed to maintain full ionisation within the plasma itself. The critical temperature between these two regimes can be simply indicated by neglecting power losses due to impurity ions and energetic atoms, so that following the analyses given in Refs.2 and 3,

$$Q_{||}^L = [A_{||}^L]_Q \, n_L v_L [(2kT_i + 4kT_e)(1 - R_E) + 2kT_e + \mathcal{E}_{DT}^{(r)} + \chi_i + \phi_w] \tag{11}$$

where the subscript L refers to conditions at $z = L_{||}$ in the lower flow channel. Here $([A_{||}^L]_Q \, n_L v_L) = \Gamma_L$ and the drift velocity v_L is equal to the ion sound speed corresponding to the temperature T_L, R_E is the energy reflection coefficient for the limiter plate, $\mathcal{E}_{DT}^{(r)}$ is the radiated energy associated with the production of a "proton"-electron pair, $\chi_i = 13.6$ eV is the ionisation threshold, and ϕ_w is the work function of the limiter surface. It is assumed in eq.(11) that secondary electrons from the limiter surface are suppressed and that all recycled particles return to the lower surfaces of the limiter. The transport equations for collisional plasma flow[2] provide the relationship to conditions at $z = 0$, namely,

$$n^L(o) \, T^L(o) = 2 \, n_L \, T_L \tag{12}$$

and, if $kT_i = kT_e = T_L$, eq.(11) becomes

$$Q^L \propto [A^L_{||}]_Q \, n^L(o) \, T^L(o) \left[T_L^{\frac{1}{2}} \left(6(1 - R_E) + 2 \right) \right.$$

$$\left. + (T_L)^{-\frac{1}{2}} (E^{(r)}_{DT} + \chi_i + \phi_w) \right]. \tag{13}$$

Accepting that both R_E and $E^{(r)}_{DT}$ tend to be invariant over the temperature range of interest yields the simple relationship that

$$Q^L_{||} \propto [A^L_{||}]_Q \, n^L(o) \, T^L(o) \, [AT_L^{\frac{1}{2}} + BT_L^{-\frac{1}{2}}] \tag{14}$$

where A and B are constants. The scrape-off temperature distant from the limiter, characterised by $T^L(o)$, tends to be invariant because of the effects of electron thermal conduction and so substitution for A and B in eq.(14) yields,

$$Q^L_{||} \propto n^L(o) \, T_L^{\frac{1}{2}} \quad [T_L \text{ greater than about 10 eV}] \tag{15}$$

$$Q^L_{||} \propto n^L(o) \, T_L^{-\frac{1}{2}} \quad [T_L \text{ less than about 10 eV}]. \tag{16}$$

Thus for a prescribed $n^L(o)$, $Q^L_{||}$ can be two valued, depending upon the regime of T_L whereas, for a prescribed $Q^L_{||}$, T_L can be two valued, depending upon the regime of $n^L(o)$.

3.3 Influence of gas exhaust upon plasma temperature at the lower surface

These differing temperature regimes can have substantial impact upon the pumping efficiency required to exhaust helium. The plasma properties within the scrape-off region are controlled by the predominant species (ie, DT) and it is convenient to consider the ratio $\Gamma^{(o)}_{DT(pump)} / Q^L_{||}$ which can be obtained from eqs.(8) and (14),

$$\frac{\Gamma^{(o)}_{DT(pump)}}{Q^L_{||}} \approx \frac{\overline{P}_{DT} F_{DT}}{(AT_L + B)} \; \frac{1}{(1 - R)_{DT}} \tag{17}$$

so that

$$T_L \approx \frac{1}{A} \left[\left(\frac{\overline{P}_{DT} F_{DT} Q^L_{||}}{\Gamma^{(o)}_{DT(pump)} (1 - R)_{DT}} \right) - B \right]. \tag{18}$$

In steady state

$$\Gamma^{(o)}_{DT(pump)} = \tfrac{1}{2} K_\alpha \left(\frac{n_{DT}}{n_{He}} \right)_o \tag{19}$$

where $K_\alpha = 2 \times 10^{20} \, s^{-1}$ is the production rate of α-particles in

INTOR and $(n_{DT}/n_{He})_o$ is the species density ratio at z = 0 within the scrape-off region. Reference to Fig.3 (in Section 5.1) shows that $\overline{P}_{DT}$ is approximately constant (ie, $\overline{P}_{DT} \approx 0.5$) over the range of interest and, since $R_{DT} \sim \overline{P}_{DT}^{\,2}$, the quantity $(1 - R)_{DT}$ is also constant. Substitution of appropriate values into eq.(18) yields

$$T_L \approx \frac{1}{6}\left[5 \times 10^4 \; F_{DT} \; Q_{||}^L \left(\frac{n_{He}}{n_{DT}}\right)_o - 45\right] \text{ (eV)} \qquad (20)$$

so that for typical conditions ($Q_{||}^L$ = 2 MW and $(n_{He}/n_{DT})_o$ = 0.05) the temperature $T_L \approx 9$ eV when F_{DT} is about 2%. Moreover, if $Q_{||}^L$ and $(n_{He}/n_{DT})_o$ can be considered as independent input parameters, then T_L is governed by the exhaust efficiency F_{DT} of DT particles.

It has been accepted throughout the INTOR workshops that the exhaust efficiencies $F_{He} = F_{DT} = F$ so that F can be determined from the exhaust rate of helium, which for the inner or outer portions of the limiter can be expressed as

$$\Gamma^{(o)}_{He(pump)} \approx \left\{\frac{\Gamma_L \overline{P} \; F}{(1 - R)}\right\}_{He} = 1 \times 10^{20} \text{ atoms s}^{-1} \; . \qquad (21)$$

The most significant aspect of this relationship is that $\overline{P}_{He}$ tends rapidly towards unity when the temperature $T_L \lesssim 10$ eV due to the inability of the cold plasma to ionise helium atoms (these effects are evident in Figs.3 and 4). Thus, when $T_L \lesssim 10$ eV, the required value of F is substantially reduced. It is thus concluded that the optimal mode of operation for the pumped limiter is in a condition where T_L is so low that the required pumping efficiency for helium is also low. The ability to achieve these twin objectives depends upon the radial characteristics of both $Q_{||}(X)$ and $n_{He}(X)/n_{DT}(X)$ within the scrape-off plasma.

4. Input Data

To date, behaviour of the upper surface of the limiter has been assessed for a density $n = 5 \times 10^{19}$ m^{-3} at the separatrix. Two surface materials have been studied, namely beryllium and tungsten. In the beryllium case the input power ($2\,Q_{\perp s}$) is taken to be 80 MW but, in view of the radiation losses associated with a limiter material of high atomic number (eg, Ref.4), the input power for tungsten is assessed over the range 10 to 80 MW. Data for the upper surfaces are

presented in tabular format so that cross reference can readily be made to the plasma characteristics predicted for a divertor configuration.[3]

The behaviour of the plasma and gas transport properties at the lower surface of the limiter plate have to be assessed for input powers $Q_{||}^{L}$ ranging from 1 to 3 MW and density $n^{L}(o)$ in the scrape-off plasma ranging from 0.5 to 2 x 10^{19} m^{-3}.

The energy-scale length specified[1] at the mid-outer-toroidal plane is taken to be $\Delta_{Q,90}$ = 1.5 cm but, in view of the uncertainties in limiter geometry and location in the poloidal plane, performance is determined only for $\Delta_{Q,\theta}$ = 6.0 cm and $R_{\theta} \approx 5.1$ m. The effects of changing $\Delta_{Q,\theta}$ are not significant *in the context of the present discussion* and the trends can be easily identified from the data previously presented for an iron limiter.[5]

5. Results

5.1 Lower surface - Tungsten

Neutral particle escape probabilities $\overline{P}_{He}$ and $\overline{P}_{DT}$ are plotted in Fig.3 against the power $Q_{||}^{L}$ that flows through the scrape-off plasma towards the lower surface of the limiter. The density $n^{L}(o)$ = 1 x 10^{19} m^{-3} is chosen as being representative of a typical mode of operation. The constancy of $\overline{P}_{DT}$ and the rapid variation in $\overline{P}_{He}$ at $Q_{||}^{L} \approx 1.7$ MW are apparent. The corresponding temperatures T_L at the lower surface and $T^{L}(o)$ in the scrape-off plasma are shown in Fig.4 and the transition between the two plasma transport modes at a temperature of about 10.0 eV is evident. The temperature difference $(T^{L}(o) - T_L)$ is approximately independent of the power flow $Q_{||}^{L}$ and this behaviour is a consequence of electron thermal conduction parallel to the magnetic field. The relative significance of the various mechanisms for power loss under the limiter plate is illustrated in Fig.5. When $T_L \gtrsim 10$ eV, the predominant loss mechanism is convective transport of DT plasma through the sheath but in the colder regime, when T_L < 10 eV, the predominant loss arises from transport of fast neutral particles to the limiter plate and torus wall. Localised radiation from DT is relatively small (< 0.1 $Q_{||}^{L}$) and that from He is even less.

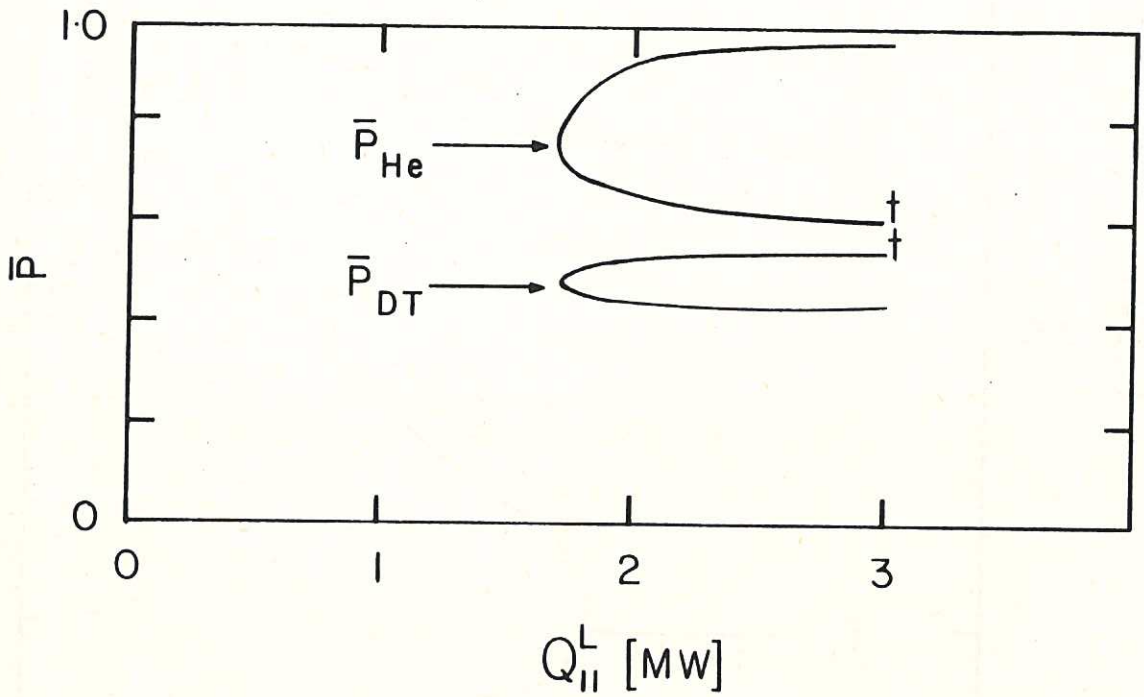

Fig.3 Escape probabilities $\bar{P}_{DT}$ and $\bar{P}_{He}$ for neutral particles released at the lower surface of a tungsten limiter plotted as functions of $Q_{\parallel}^{L}$, the power flowing towards the surface.
The symbol † identifies the high temperature region (i.e. $T_L > 10$eV).
Data refer to:

scrape-off plasma density	$n^L(o) = 1 \times 10^{19}\ m^{-3}$
effective area of flow channel	$[A_{\parallel}^{L}]_Q = 0.145$m
radial scale length for energy transport	$\Delta_{Q,\theta} = 6$cm
ion species ratio in the scrape-off	$(n_{He}/n_{DT})_o = 5\%$
charge state of impurity ion Z = 4	

Analyses are performed for a drift length $L_{\parallel}$ equal to half the length of the magnetic flux tube which links the limiter plates. The total power flow to the "inner" and "outer" portions of the lower surface is thus $2Q_{\parallel}^{L}$.

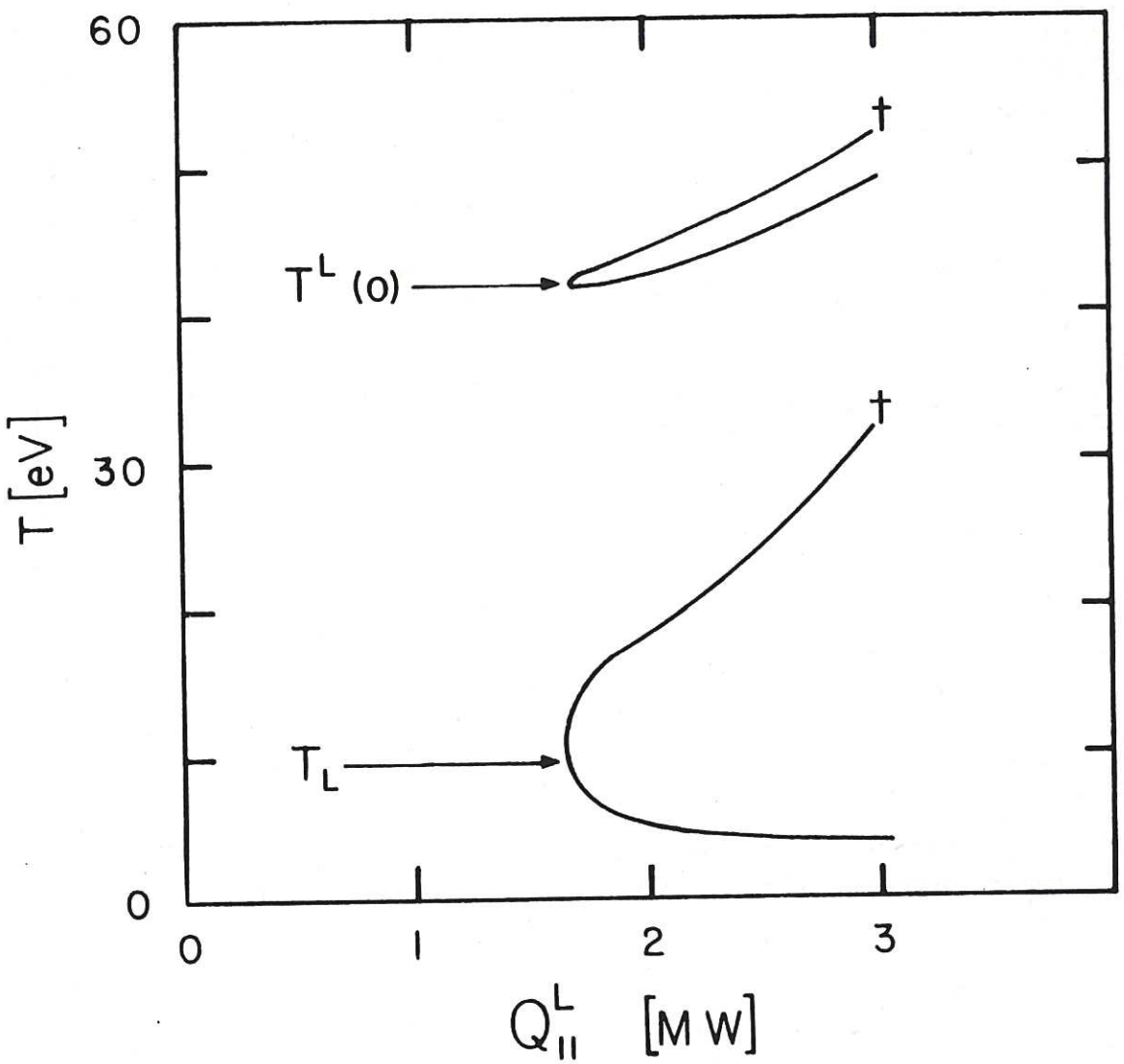

Fig.4 Temperature in the scrape-off plasma $T^L(o)$ and at the sheath edge T_L plotted as a function of the power flow, $Q_{\parallel}^L$, towards the lower surface of a tungsten limiter plate. Plasma conditions are the same as for Fig.3.

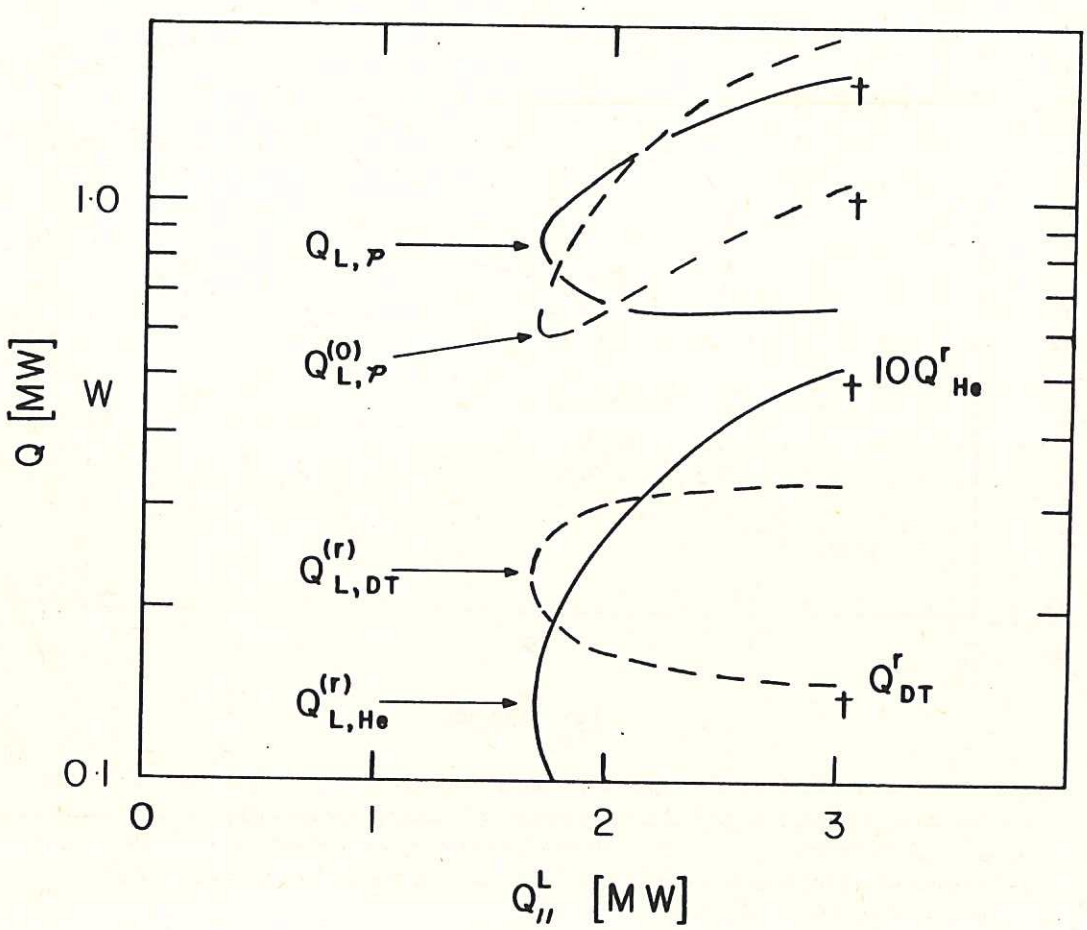

Fig.5 Power transport in the plasma flow to the lower surface of a tungsten limiter plate.

$Q_{L,P}$ is the power convected to the surface by DT and He plasma

$Q^{(o)}_{L,P}$ is the power transported by energetic DT and He atoms to the torus wall and to the limiter plate

$Q^{(r)}_{L,DT}$ is the radiative power losses from DT

$Q^{(r)}_{L,He}$ is the radiative power losses from He

Losses from tungsten are less than 10^{-3} $Q^{L}_{\parallel}$. Plasma conditions are the same as for Fig.3.

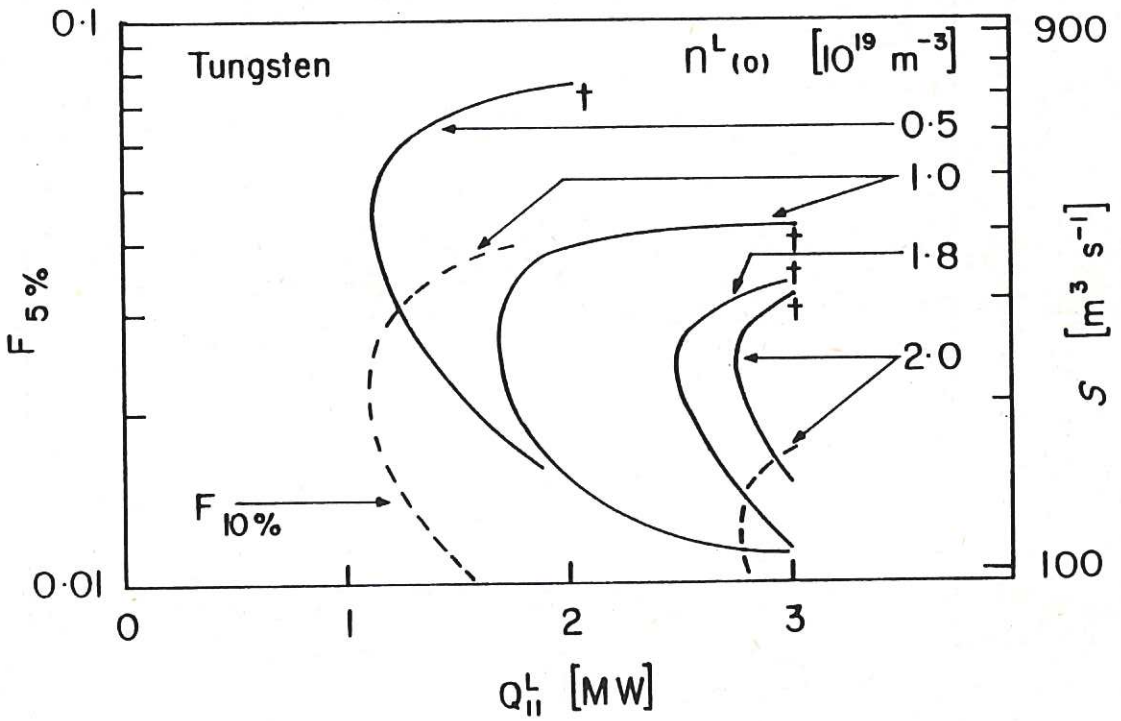

Fig.6 The exhaust efficiency $F_{5\%}$ required to maintain $(n_{He}/n_{DT})_o$ = 5% plotted as a function of the power, $Q_{\parallel}^L$, flowing towards the lower surface of a tungsten limiter plate.
The speed of the vacuum pumps S is assessed for the cassette geometry described in Ref.3 and on the assumption that both the inner and outer portions of the limiter contribute equally to the flow of neutral particles to the ducts.
The dashed curves show the values of $F_{10\%}$ required to maintain $(n_{He}/n_{DT})_o$ = 10%.
Data refer to: effective area of flow channel $[A_{\parallel}^L]_Q = 0.145\,m^2$
radial scale length for energy transport $\Delta_{Q,\theta}$ = 6cm.

Local power losses due to sputtered tungsten impurities are insignificant, they do not exceed $\sim$ 1 kW.

Variation of $F_{5\%}$ (the exhaust efficiency required to maintain $(n_{He}/n_{DT})_o$ = 5%) is plotted in Fig.6 against $Q_{||}^L$ and the two valued nature of the solutions predicted by the model are apparent. The conclusion to be drawn is that the pumping efficiency $F_{5\%}$ tends towards a constant value of about 1% when $Q_{||}^L$ is about 3 MW, and it is fortunate that this is compatible with a peak power loading at the tip of $\approx$ 1 MW m^2. When F $\approx$ 1%, then the exhaust requirements at 3 MW are rather insensitive to the scrape-off density $n^L(o)$. Some data for $(n_{He}/n_{DT})_o$ = 10% are shown and it is apparent that $F_{10\%}$ tends to $\frac{1}{2}$ $F_{5\%}$ when T_L is in the low temperature regime. This is to be expected from the behaviour outlined in Section 3.3.

The speed S_{300K} of the *vacuum pumps* required to attain these values of F is estimated for the cassette duct geometry described in Ref.3 using the assumption that both the inner and outer portions of the divertor plate contribute equally to pumping. If $F_{5\%}$ lies in the range 1 to 1.5×10^{-2} (ie, as predicted for $Q_{||}^L$ = 3 MW and $n^L(o)$ in the range 0.5 to 2×10^{19} m^{-3}) then the corresponding speeds are S_{300K} = 100 to 150 m^3 s^{-1}.

5.2 Lower surface - Beryllium

Data for $F_{5\%}$ in the case of the beryllium limiter are shown in Fig.7. The dependence of $F_{5\%}$ upon the power flow $Q_{||}^L$ exhibits the same trends as that for the tungsten limiter but the corresponding magnitude of $F_{5\%}$ is almost twice that predicted for tungsten. This fact arises because the energy and particle reflection coefficients for DT and He incident upon a beryllium surface are relatively low and so a greater proportion of cold neutral particles is released at the beryllium limiter and these particles escape less readily from the plasma channel. When $Q_{||}^L \approx$ 3 MW and $n^L(o) \leqslant 1.5 \times 10^{19}$ m^{-3}, the values of $F_{5\%}$ converge to about 1.6% and $S_{300K} \approx 150$ m^3 s^{-1}. For $n^L(o) = 2 \times 10^{19}$ m^{-3} the power flow must be higher to attain convergence, say about 4 MW.

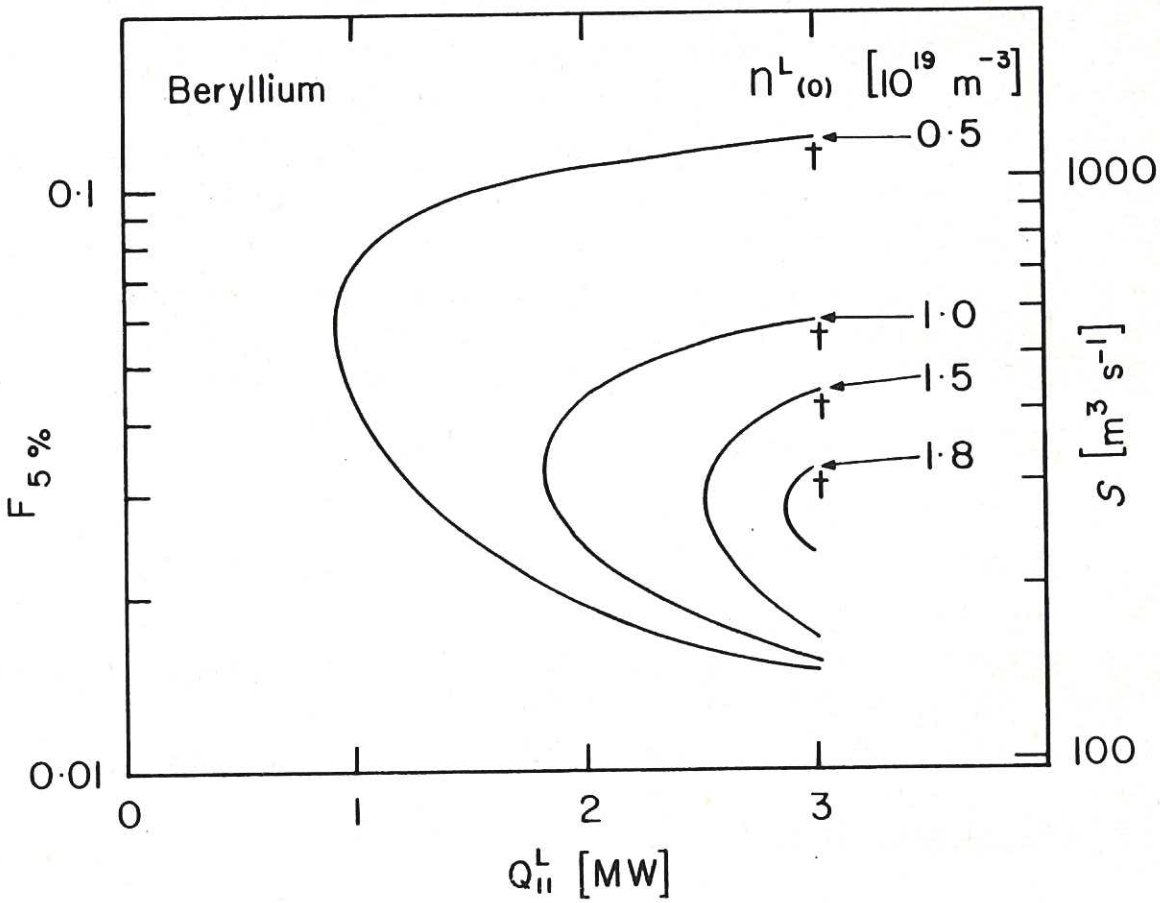

Fig.7 The exhaust efficiency $F_{5\%}$ and the speed of the vacuum pumps S required to maintain $(n_{He}/n_{DT})_o$ = 5% in the case of a beryllium limiter plate.
Plasma and gas exhaust parameters are the same as those in Fig.6.

Input Power 2 $Q_{\perp s}$ [MW]	80			40			20			10		
Charge State of Recycling W Ions	3	4	5	3	4	5	3	4	5	3	4	5
Temp. of scrape-off; $T^U(o)$ [eV]	*119*	*115*	*113*	95	95	*94*		74			59	
Temp. at limiter plate; T_U [eV]	*65*	*49.3*	*39.5*	44	44	*39*		17.5			6	
Flow of DT and He ions to plate; $\Gamma_{U,P}$ [$10^{23}s^{-1}$]	*4.3*	*5.2*	*5.4*	4.0	4.0	*4.2*		4.5			4.6	
Flow of DT and He atoms across the separatrix; $\Gamma^{(o)}_{s,P}$ [$10^{22}s^{-1}$]	*5.5*	*4.5*	*3.9*	4.3	4.3	*4.0*		2.8			4.0	
Flow of DT and He atoms to the limiter plate; $\Gamma^{(o)}_{U,P}$ [$10^{22}s^{-1}$]	*3.3*	*3.2*	*3.3*	2.8	2.8	*2.8*		2.8			4.2	
Power to plate carried by DT and He ions; $Q_{U,P}$ [MW]	*27.8*	*23.2*	*21.5*	16.8	16.6	*15.8*		7.2			3.0	
Power to plate carried by tungsten ions; $Q_{U,W}$ [MW]	*5.9*	*8.8*	*9.3*	0.03	0.11	*0.65*		3.10^{-5}			0	
Power radiated by DT and He; $Q^{(r)}_{U,P}$ [MW]	*0.77*	*0.85*	*0.88*	0.69	0.70	*0.74*		0.75			0.7	
Power radiated by tungsten; $Q^{(r)}_{U,W}$ [MW]	*2.7*	*4.5*	*5.4*	0.03	0.07	*0.40*		$<10^{-4}$			0	
Net power carried inboard of the separatrix by atoms; $Q^{(o)}_s$ [MW]	*3.3*	*1.65*	*0.72*	1.7	1.5	*1.1*		- 0.2			- 0.9	
Sputter rate of W; $\Gamma^{(o)}_W$ [$10^{22}s^{-1}$]	*3.17*	*4.65*	*4.90*	0.027	0.067	*0.345*	0	$<10^{-4}$	$<10^{-4}$		0	
Erosion rate of W; ξ_W [μmh^{-1}]	*85*	*130*	*130*	0.73	1.8	*9.4*	0	< 0.01	< 0.01		0	
Tip displacement; $\hat{X}$ [m]		0.186			0.144			0.103			0.061	
Effective flow area; $[A^U_{\parallel}]_Q$ [m^2]		0.14			0.13			0.12			0.085	

TABLE 1 Predicted performance of the upper surface of the inner or outer portions of a tungsten limiter plate

Data are assessed on the assumption:

1. That the input flow 2 $Q_{\perp s}$ is equally distributed to the inner and outer portions of the plate.
2. The total area of the upper surface of the plate is assumed to be 40 m^2.
3. The displacement of the tips $X_t \approx \hat{X}$ is adjusted for each value of $Q_{\perp s}$ so that the peak power loading close to the tip is $\approx$ 1 MW/m^2.
4. The scrape-off density $n_s = 5 \times 10^{19}\ m^{-3}$.
5. The effective flow area $[A^U_{\parallel}]_Q = 0.145\ [1 - \exp(\hat{X}/\Delta_{Q,\theta})]$
6. The energy scale length $\Delta_{Q,\theta} = 0.06$ m.
7. The ion species ratio in the scrape-off plasma $(n_{He}/n_{DT})_o = 5\%$.

Conditions where the plasma temperature close to the limiter is regulated by self-sputtering are shown by underlined *script type-face*

Input Power $2\,Q_{\perp s}$ [MW]			80	
Charge State of Recycling Be Ions			3	4
Temp. of scrape-off;	$T^U(o)$	[eV]	113	112
Temp. at limiter plate;	T_U	[eV]	41	33
Flow of DT and He ions to plate;	$\Gamma_{U,P}$	$[10^{23}s^{-1}]$	5.2	5.8
Flow of DT and He atoms across the separatrix;	$\Gamma^{(o)}_{s,P}$	$[10^{22}s^{-1}]$	2.5	2.3
Flow of DT and He atoms to the limiter plate;	$\Gamma^{(o)}_{U,P}$	$[10^{22}s^{-1}]$	3.3	3.6
Power to plate carried by DT and He ions;	$Q_{U,P}$	[MW]	28.2	27.6
Power to plate carried by beryllium ions;	$Q_{U,Be}$	[MW]	8.3	9.0
Power radiated by DT and He;	$Q^{(r)}_{U,P}$	[MW]	0.95	1.00
Power radiated by beryllium;	$Q^{(r)}_{U,Be}$	[MW]	0.03	0.02
Net power carried inboard of the separatrix by atoms;	$Q^{(o)}_s$	[MW]	0.15	- 0.15
Sputter rate of Be;	$\Gamma^{(o)}_{Be}$	$[10^{22}s^{-1}]$	7.0	7.1
Erosion rate of Be;	ξ_{Be}	$[\mu mh^{-1}]$	100	100
Tip displacement;	$\hat{X}$	[m]	0.186	
Effective flow area;	$[A^U_{\parallel}]_Q$	$[m^2]$	0.14	

TABLE 2 Predicted performance of the upper surface of the inner or outer portions of a beryllium limiter plate for a total input power $2Q_{\perp s}$ = 80 MW.

Description of the relevant plasma and configurational parameters are given in Table 1.

5.3 Upper surface - Tungsten

Predicted behaviour of the upper surface of a tungsten limiter is presented in Table 1. The density of plasma at the separatrix is taken to be 5×10^{19} m^{-3} and the input power $2\ Q_{\perp s}$ ranges from 10 to 80 MW. The highest tabulated power is probably unphysical due to tungsten radiation losses inboard of the separatrix but it is included to permit ready comparison of the scrape-off plasma characteristics predicted for tungsten and beryllium limiters. The power flow $Q_{U,P}$ to the plate includes an allowance $Q_s^{(o)}$ due to power recirculated across the separatrix by atoms released from the plate but in all cases of interest $Q_s^{(o)} << Q_{\perp s}$.

Self-sputtering is assessed (as in Ref.3) using the assumption that the recycling ions are either W^{3+}, W^{4+} or W^{5+} and with the exception of W^{5+} (at 40 MW) regulation of the sheath temperature at the self-sputter limit does not occur when $2\ Q_{\perp s} \leqslant 40$ MW. The power dissipated by tungsten impurities ($Q_{U,W}^{(r)} + Q_{U,W}$) within the immediate locality of the sheath is relatively low and it is important to note that about 1 MW is sufficient to provide temperature regulation at the sputter limit of W^{5+} when $Q_{\perp s} = 40$ MW. This behaviour is a consequence of the powerful flow of DT which recycles to the limiter plate and the reasons are discussed in Ref.3.

Sputter erosion of the limiter plate is likely to be small provided $Q_{\perp s} \lesssim 40$ MW and radial modelling[4] indicates that $Q_{\perp s} \approx 40$ MW is a reasonable assumption for a tungsten limiter. Provided the predominant charge state of recycling tungsten does not exceed $Z = 4$, then the sputter rate of the plate is negligible at 40 MW (< 4 mm per year at 25% availability) and only rises to 2 cm per year for W^{5+}. The average temperature of the scrape-off plasma at 40 MW is about 95 eV.

5.4 Upper surface - Beryllium

Data for the upper surface of a beryllium limiter are presented in Table 2 for an input power of 80 MW and self-sputtering by Be^{3+} and Be^{4+} ions. The sputtering of the limiter is substantial (22 cm per year when redeposition is neglected) and about 10% of the input power $Q_{\perp s}$ is carried through the sheath by multiply-charged Be ions. In contrast, atomic radiation losses due to Be ions which recycle to the

limiter are negligible. There is also negligible recirculation of power across the separatrix by energetic atoms released at the plate because of the weak backscattering efficiency of a beryllium surface.

6. Conclusions

The present modelling predicts that the helium exhaust requirements of INTOR can be attained by the pumped limiter configuration envisaged in Phase IIA. The exhaust efficiency is very comparable to that of the single-null divertor (ie, pumps of speed about 100 $m^2\ s^{-1}$ being required) provided that the power flow to the lower surface of the plate, $2Q_{||}^{L}$, is not less than 6 MW. It is particularly fortunate that this power flow is comparable with a limiter tip power loading of about 1 MW/m^2 in the geometry envisaged for INTOR.

Two operating regimes are predicted, depending on the plasma temperature close to the lower surface of the plate; transition between one regime and the other is dependent upon the exhaust efficiency of the system (ie, the pump speed and the geometry of the gas ducts). The validity of these predictions depends upon the radial characteristics of the power flow $Q_{||}(X)$ parallel to the magnetic field within the scrape-off plasma and also upon the radial characteristics of the density ratio $[n_{He}(X)/n_{DT}(X)]$ within the scrape-off. Neither of these properties is assessed in a self-consistent manner, indeed they are used as prescribed inputs to the model.

The parameter space selected for the present study of the scrape-off and limiter plasma is based largely upon predictions of radial transport codes because the parallel transport models do not allow for atomic losses inboard of the separatrix or for atomic losses associated with plasma transport in regions of the scrape-off layer which are distant from the limiter. However, these omissions are not of themselves likely to invalidate the analysis because:

a. In the case of tungsten, impurity radiation losses occur predominantly inboard of the separatrix and the concentration of impurity ions throughout the scrape-off plasma is likely to be low.[4] The radiation losses can be allowed for by appropriate selection of $Q_{\perp s}$ and it is reasonable to neglect the

presence of tungsten ions when assessing energy transport by charged particles along the scrape-off plasma.

b. In the case of beryllium, radiation losses are likely to be distributed predominantly within the scrape-off plasma where the concentration of impurity ions may be significant. However, these ions are light and lowly charged and therefore they are unlikely to influence substantially the transport properties of the DT plasma. Radiation and atomic losses can again be allowed for by selection of $Q_{\perp s}$.

The modelling indicates some general trends in behaviour. There is evidence that DT recycles powerfully in the immediate vicinity of the limiter plate when the scrape-off density $n(o) > 10^{19}\ m^{-3}$. This can be identified by the relatively small probability for the escape of atoms from the upper surface of the limiter to the separatrix. For example, the localised recycling coefficient can be expressed as $\left[1-\left(\Gamma_{s,P}/\Gamma_{U,P}\right)\right]$ which from Table 1 has a value of about 0.9. Such localised recycling is maintained by charged particle energy transport and, typically, a minimum of 4 MW is required to maintain a scrape-off density of $10^{19}\ m^{-3}$ (see, for example, conditions of $T_L \approx 10$ eV shown in Fig.4). The energy is transported by electron conduction along the magnetic flux tubes and so an appreciable temperature gradient exists between the localised sheath at the limiter and the bulk of the scrape-off plasma. The average temperature at the separatrix is therefore unlikely to be less than about 50 eV, indeed it may be greater due to the power flow needed to sustain recycling at the torus wall (this component is neglected in the present treatment). The power flow needed to sustain DT plasma density within the scrape-off region increases when the sheath temperature exceeds 10 eV due to the increasingly predominant role of convective energy transport through the sheath. Radiative power losses arising from acceptable concentrations of impurity ions within the volume of the scrape-off plasma are in all conditions appreciably less than the energy transported by the DT component of the plasma. Thus to cool the scrape-off plasma by impurity radiation it is first necessary for the impurities to penetrate the separatrix and thereby

establish an inboard radiative edge which reduces the DT plasma power flow entering the scrape-off region.

These predicted characteristics are broadly compatible with the results for both carbon and iron limiters determined using a radial transport code coupled to a simplified scrape-off model (Ref.4). Comparable simulations (Ref.8) seek to reduce wall and limiter sputtering by lowering the overall temperature of the scrape-off plasma to about 10 eV. In these conditions both the power flow and density in the scrape-off plasma must be very low (and this is compliant with the present predictions) but such conditions are incompatible with the helium exhaust requirements of INTOR.

References

1. Conclusions from the 5th meeting of the INTOR Phase IIA Workshop, IAEA Vienna (Euratom, EURFUBRU/XII-132/82/EDV24, Brussels 1982).

2. Harrison M F A, Harbour P J and Hotston E S (1981). In "European contributions to the Conceptual Design of the INTOR Phase I Workshop", Euratom, EURFUBRU/XII-132/82/EDV2, Brussels (1982) p.231. In course of publication, Nuclear Technology/Fusion.

3. Harrison M F A and Hotston E S (1982). In "European contributions to the INTOR Phase IIA Workshops" Chapter VI.3 Appendix 3. Also Culham Report CLM-R226.

4. Neuhauser J, Lackner K and Wunderlich R (1982). In "European contributions to the INTOR Phase IIA Workshops" Chapter VI.2.4 Appendix 1.

5. Harrison M F A and Hotston E S (1982). In "European contributions to the 4th meeting of the INTOR Phase IIA Workshop, IAEA Vienna (Euratom, EURFUBRU/XII-132/82/EDV13, Brussels 1982).

6. Harrison M F A and Hotston E S (1982). In "European contributions to the 5th meeting of the INTOR Phase IIA Workshop, IAEA Vienna (Euratom, EURFUBRU/XII-132/82/EDV20, Brussels 1982).

7. Gruber O and Lackner K (1982). In "European contributions to the INTOR Phase IIA Workshops" Chapter IX.2.1/2.2.

8. Abels van Maanen A E P M and Watkins M L (1982). In "European contributions to the INTOR Phase IIA Workshops" Chapter VI.2.4 Appendix 2.

HER MAJESTY'S STATIONERY OFFICE

Government Bookshops

49 High Holborn, London WC1V 6HB
(London post orders: PO Box 569, London SC1 9NH)
13a Castle Street, Edinburgh EH2 3AR
41 The Hayes, Cardiff CF1 1JW
Brazennose Street, Manchester M60 8AS
Southey House, Wine Street, Bristol BS1 2BQ
258 Broad Street, Birmingham B1 2HE
80 Chichester Street, Belfast BT1 4JY

Publications may also be ordered through any bookseller